# Anisotropic self-diffusion in thermotropic liquid crystals studied by $^{1}H$ and $^{2}H$ pulse-field-gradient spin-echo NMR

S. V. Dvinskikh,[1],* I. Furó,[2] H. Zimmermann,[3] and A. Maliniak[1]
[1]*Division of Physical Chemistry, Arrhenius Laboratory, Stockholm University, SE-10691 Stockholm, Sweden*
[2]*Division of Physical Chemistry, Department of Chemistry, Royal Institute of Technology, SE-10044 Stockholm, Sweden*
[3]*Department of Biophysics, Max-Planck-Institut für Medizinische Forschung, D-69120 Heidelberg, Germany*

(Received 25 January 2002; published 10 June 2002)

The molecular self-diffusion coefficients in nematic and smectic-*A* thermotropic liquid crystals are measured using stimulated-echo-type $^{2}H$ and $^{1}H$ pulse-field-gradient spin-echo nuclear magnetic resonance (PGSE NMR) combined with multiple-pulse dipolar decoupling and slice selection. The temperature dependence of the principal components of the diffusion tensor in the nematic phase follows a simple Arrhenius relationship except in the region of nematic-isotropic phase transition where it reflects, merely, the decrease of the molecular orientational order. The average of the principal diffusion coefficients in the isotropic-nematic phase transition region is close to the diffusion coefficient in the isotropic phase. At the nematic–smectic-*A* phase transition the diffusion coefficients change continuously. The results in nematic phase are best described in terms of the affine transformation model for diffusion in nematics formed by hard ellipsoids. In the smectic-*A* phase the data are interpreted using a modified model for diffusion in presence of a periodic potential along the director.

DOI: 10.1103/PhysRevE.65.061701 PACS number(s): 61.30.−v, 66.10.Cb, 82.56.Lz, 76.60.−k

## I. INTRODUCTION

Anisotropic translational diffusion in thermotropic liquid crystals (LC) has attracted considerable attention in the past. This information is essential for understanding various aspects of the anisotropic molecular interactions and ordering in mesophases [1–6]. Diffusion in LCs has been studied by a variety of experimental techniques including quasielastic neutron scattering (QENS), magnetic resonance [electron spin resonance (ESR) and nuclear magnetic resonance (NMR)], forced Rayleigh scattering (FRS), optical microscopy, and radioactive tracer diffusion. To date, a general understanding of the relationship between the diffusion processes and the orientational order in various types of thermotropic liquid crystals has been reached. Further progress in revealing the details of molecular diffusion, however, has been limited due to experimental problems. In particular, there is a lack of data in phase transition regions that are reliable enough to be confronted with theoretical models.

Recently, we have reported new pulsed-field-gradient spin-echo (PGSE) NMR experiments that enable accurate measurements of diffusion coefficients in anisotropic systems, such as LCs or soft solids [7–12]. Compared to other methods, PGSE NMR is unique because it is noninvasive, molecularly selective, and requires no foreign probes [1,3,13–18]. In this technique, no change of molecular properties is required, instead, the uniform labeling of the position of all molecules in the sample is achieved by spatial encoding of the NMR resonance frequency in the presence of the magnetic field gradient. The method in its original form is, however, less suitable for liquid crystalline materials where anisotropic spin interactions, such as the nuclear dipole-dipole coupling, are not averaged to zero by molecular motions. Hence, spin coherences created by radio-frequency pulses decay quickly, which leaves insufficient time for the encoding/decoding gradient pulses [1,3]. Our approaches are based on the early concept of combining the $^{1}H$ multiple-pulse dipolar decoupling and the PGSE technique [19–24]. Furthermore, a PGSE experiment, which involves deuterium stimulated echo sequence, was recently developed [12] and used to determine the slow molecular diffusion ($\sim 10^{-14}$ m$^2$/s) in a columnar, liquid crystalline phase [25]. For LCs with molecular diffusion coefficients $>10^{-12}$ m$^2$/s these new experiments provide the diffusion coefficients with an accuracy of few percents, as demonstrated on lyotropic [7–10] and thermotropic [11,12] liquid crystals.

In the present work, we extend our previous investigations of thermotropic nematic phases. In addition, we report diffusion measurements in a smectic-*A* phase. We focus here on the analyses of the experimental diffusion coefficients and, in particular, their correspondence to different dynamical models for both nematic and smectic phases.

The paper is organized as follows: in Sec. II experimental details are provided, the main features of the diffusion models are presented in Sec. III. Finally, the experimental results and validity of the various models are discussed in Sec. IV.

## II. EXPERIMENT

The measurements were performed on three thermotropic liquid crystals formed by ethoxy-benzylidene-butyl-aniline (EBBA), 4-pentyl-4′-cyanobiphenyl (5CB), and partially deuterated 4-octyl-4′-cyanobiphenyl (8CB). The EBBA sample was obtained from NIOPIK, St. Petersburg. The sample of 5CB was a kind gift from Merck, UK. The 8CB

---

*Corresponding author; Electronic address: sergey@physc.su.se; on leave from the Institute of Physics, St. Petersburg State University, 198904 St. Petersburg, Russia.

sample, synthesized according to previously described procedure [26], was deuterated in all positions except the $\beta$-CH$_2$ group of the aliphatic chain. All samples were used without further purification. The phase transition temperatures, estimated from NMR spectra and by polarizing microscopy, were in agreement with previously tabulated values [27]. Both nematic and smectic phases orient homogeneously with the director parallel to the external magnetic field of the NMR spectrometer. The measurements were performed on a Bruker DMX-200 spectrometer (4.6 T), operating at 200, 50, and 31 MHz for $^1$H, $^{13}$C, and $^2$H nuclei, respectively. A home-built multiple-tuned gradient probe was used [8,28]. The probe was equipped with two interchangeable gradient coils that produced magnetic field gradients either along the $z$ (parallel to $B_0$) or $x$ (perpendicular to $B_0$) axes [28]. The length of the 90° radio-frequency pulses were 2.3, 7.0, and 5.0 $\mu$s for $^1$H, $^{13}$C, and $^2$H, respectively. The gradient coils were calibrated by measuring the diffusion coefficients of D$_2$O in the temperature range of 5–45 °C by $^2$H PGSE NMR and comparing them to literature data [29]. The sample temperature was stable and reproducible within $\pm 0.15$ K. Sample heating by the decoupling sequences was estimated by observing the shift in the isotropic-nematic transition temperature and the recycling delay was adjusted to keep the heating effect to less than 0.4 K. The typical random error of the diffusion coefficient values, estimated from the reproducibility, were about $\pm 2\%$ near the phase transition to isotropic phase and $\pm 5\%$ at the lowest temperatures.

The diffusion in the *isotropic* phase was measured by conventional Hahn-echo or stimulated-echo-type PGSE NMR [13,14]. In the mesophase of protonated samples 5CB and EBBA most of the data were obtained by $^1$H PGSE NMR combined with *homonuclear* multiple-pulse dipolar decoupling [8], while a few points were also measured by the *heteronuclear* $^{13}$C{$^1$H} analog of this technique [7] and by method based on $^1$H magic-echo [24]. In the partially deuterated 8CB sample most of the measurements were performed by stimulated-echo-type $^2$H PGSE NMR on the signal from the methyl group [12] with supplementary experiments by $^1$H homonuclearly decoupled PGSE NMR on the signal from the $\beta$-CH$_2$ group.

## III. DIFFUSION MODELS

In this section, a number of theoretical models for molecular diffusion in the nematic and smectic phases will be discussed. For the former, three different approaches are compared: (i) a model based on a properly parametrized form of the velocity correlation function proposed by Chu and Moroi [30], (ii) an affine transformation model suggested by Hess *et al.* [31], and (iii) a hydrodynamic approach developed by Franklin [32]. In the smectic phase the modified model of Volino and co-workers [33,34] for diffusion in the presence of a periodic potential will be considered.

While many models have been described in the literature, those selected here have already been used by other authors for interpreting experimental diffusion results in LCs and some have been tested using molecular dynamics simulation.

### A. Nematic phase

*Chu and Moroi (CM) model*. The self-diffusion coefficient in nematic phases has been derived via a parametrized form of the linear momentum time autocorrelation function in the limit of perfectly ordered clusters [30]. The theory relates $D_\parallel$ and $D_\perp$, the principal components of the diffusion tensor parallel and perpendicular to the phase director, to the uniaxial molecular geometry and the order parameter $S$ by

$$D_\parallel = \langle D\rangle[1+2S(1-\rho)/(2\rho+1)] \tag{1a}$$

and

$$D_\perp = \langle D\rangle[1-S(1-\rho)/(2\rho+1)], \tag{1b}$$

with the *isotropic average* defined by

$$\langle D\rangle = (2D_\perp + D_\parallel)/3, \tag{1c}$$

where $\rho=\pi/(4Q)$ is a geometrical factor for a rodlike molecule of length $L$ and diameter $d$ with the axial ratio $Q = L/d$. The theory predicts that the isotropic average is independent of $S$ and at the transition to the isotropic phase (i.e., in the limit $S\rightarrow 0$) coincides with $D_{iso}$, the diffusion coefficient in the isotropic phase. Consequently, $\langle D\rangle$ is supposed to follow the temperature dependence extrapolated from the diffusion coefficients in the isotropic phase, with no discontinuity at the isotropic-nematic phase transition. The model has been previously applied with varying success to nematic liquid crystals: $p$-azoxyanisole (PAA) [30,35], 5CB [11,36], and methoxy-benzylidene-butyl-aniline (MBBA) [21,35,37]. Particularly, some agreement with the radio-tracer results in PAA was found [30].

*Hess-Frenkel-Allen (HFA) model*. The following expressions have been obtained for the diffusion in nematic phase by the affine transformation from the isotropic diffusion of hard spheres to the space of aligned uniaxial ellipsoids [31]:

$$D_\parallel = \langle D\rangle_g \alpha[Q^{4/3} - 2/3Q^{-2/3}(Q^2-1)(1-S)] \tag{2a}$$

and

$$D_\perp = \langle D\rangle_g \alpha[Q^{-2/3} + 1/3Q^{-2/3}(Q^2-1)(1-S)], \tag{2b}$$

where

$$\alpha = [1+2/3(Q^{-2}-1)(1-S)]^{-1/3}[1+1/3(Q^2-1) \times(1-S)]^{-2/3} \tag{2c}$$

for a molecule with axial ratio $Q$. Note that according to this model the isotropic average $\langle D\rangle$, as defined in Eq. (1c), is sensitive to the molecular orientational order and geometry. Instead, the *geometric average*

$$\langle D\rangle_g = (D_\perp^{2/3} D_\parallel^{1/3}) \tag{2d}$$

is predicted to be independent of the molecular shape and order and becomes $D_{iso}$ at $S=0$. This model has been successfully tested using molecular dynamics computer simulation [31,38] and also recently by comparison to NMR results [11].

*Franklin model*. The model is based on the hydrodynamic theory for isotropic liquids and the diffusion coefficients are defined by the following expressions [32]:

$$D_{\parallel} = kT[1/\mu f + (2+S)/(6\pi\mu^2\Phi\alpha_{\parallel})] \tag{3a}$$

and

$$D_{\perp} = kT[1/\mu f + (5-S)/(12\pi\mu^2\Phi\alpha_{\perp})], \tag{3b}$$

where $k$ is the Boltzmann's constant, $f$ is the scalar friction constant, $\mu$ and $\Phi$ are geometrical parameters related to the molecular structure. Viscosity parameters $\alpha_{\parallel}$ and $\alpha_{\perp}$ are given by the linear combination of five Leslie coefficients $\alpha_i$, $i=1-5$ (for the explicit formulas see the original paper [32] and also the correction by Urbach *et al.* [35]).

Apparently, the temperature dependence of the anisotropic radio-tracer diffusion in the nematic phase of PAA was correctly predicted using this model [32]. The theory involves many parameters (friction and viscosity constants), which are often not readily available with sufficient accuracy. Therefore, the analysis using this model is not always feasible. In the present work we restrict it to 5CB, for which the required material properties have been reported elsewhere.

### B. Smectic-*A* phase

Volino and co-authors [33,34] have modeled the diffusion in smectic-*A* phase with the assumption of the existence of periodic potential along the smectic director. This creates a potential barrier, which influences the molecular diffusion along the director ($z$ coordinate), while the in-layer diffusion remains essentially unaffected. Thus, the temperature-independent symmetric potential becomes

$$V = -V_1/2\cos(2\pi z/d) \tag{4}$$

where $d$ is the layer spacing. With this potential, the equations for the diffusion in smectic-*A* phase are given by

$$(D_{\parallel})^{sm} = (D_{\parallel})^{nem}[I_0(V_1/2RT)]^{-2} \tag{5a}$$

and

$$(D_{\perp})^{sm} = (D_{\perp})^{nem}, \tag{5b}$$

where $I_0$ is the modified Bessel function of first kind and of zero order, $(D_{\parallel})^{nem}$ and $(D_{\perp})^{nem}$ are the diffusion coefficients in the absence of smectic positional ordering but in presence of the nematic orientational order. For the nonzero potential amplitude $V_1$ this model predicts discontinuity of $D_{\parallel}$ at the nematic–smectic-*A* phase transition. This approach has successfully described the diffusion measured by QENS and NMR methods in some smectic LCs with a pronounced discontinuity of $D_{\parallel}$ at the nematic-smectic phase transition [1,39].

## IV. RESULTS AND DISCUSSION

The results of diffusion experiments in isotropic and liquid crystalline phases for 5CB, 8CB, and EBBA samples are collected in Figs. 1 and 2.

In the nematic and smectic-*A* liquid crystals the second-rank diffusion tensor has, due to the uniaxial symmetry of the liquid crystals, two principal values. Since the director is homogeneously oriented along the magnetic field of the spectrometer, the two principal diffusion coefficients $D_{\parallel}$ and $D_{\perp}$ are measured by magnetic field gradient held, respectively, parallel and perpendicular to the main magnetic field. In the isotropic phase the experimental diffusion coefficients for the two gradient directions coincide.

### A. Isotropic and nematic phases

The molecular diffusion in isotropic and nematic phases of the three compounds exhibits some common qualitative features that can be observed in Fig. 1, and summarized as follows: (i) temperature dependence of the diffusion coefficient in the isotropic phase exhibits Arrhenius-type behavior with $D = D_0\exp(-E_a^{iso}/RT)$, (ii) the relation $D_{\parallel} > D_{\perp}$ holds for all liquid crystalline phases; (iii) the diffusion in nematic phase, except in the phase transition region, can be approximated using Arrhenius relationship with $E_a^{\parallel} < E_a^{iso} < E_a^{\perp}$, and (iv) the diffusion coefficients in the liquid crystalline and isotropic phases are related by $D_{\parallel} > D_{iso} \approx \langle D\rangle \approx \langle D\rangle_g > D_{\perp}$, where $D_{iso}$ is extrapolated from the isotropic phase and $\langle D\rangle$, $\langle D\rangle_g$ are the average diffusion coefficients as defined in Eqs. (1c) and (2d). This contrasts some previous unexpected observations where $D_{\parallel}, D_{\perp} > D_{iso}$ and $D_{\parallel}, D_{\perp} < D_{iso}$. Such results obtained by foreign probe molecules [1,40–45] may be connected to their different mass and geometry, while data obtained on the mesogenic molecules [2,21,46] may rather be attributed to experimental artifacts.

The diffusion anisotropy $D_{\parallel}/D_{\perp}$ shown in Fig. 3(a) is largest in EBBA; it varies from 1.8 at the phase transition to ≈3.3 at low temperatures. For 5CB, the corresponding values are 1.6 and 2.7, respectively. In 8CB, the anisotropy reaches a maximum value of ≈2.1 in the nematic phase and decreases to ≈1.7 on further cooling in the smectic phase.

The activation energies *in the isotropic phase* for 5CB, 8CB, and EBBA are collected in Table I. They agree, in general, well with other NMR results [4,5,46–55]. Due to the methodical difficulties, the diffusion coefficients obtained by different methods *in the nematic phase* differ by as much as one order of magnitude. For 5CB, the literature diffusion data in the isotropic and nematic phase have been compiled in Ref. [11]. Recent measurement of diffusion (only $D_{\parallel}$) in these phases of 5CB by stray field static gradient NMR [54] agree well with our results. Also, deuteron magic-echo PGSE NMR [12] measurements performed recently in chain deuterated 5CB-$d_{11}$ [76] confirmed our previous proton data [11]. For 8CB, the diffusion coefficients obtained by FRS technique on probe molecules [44] are underestimated by a factor of up to 2 and the observed diffusion anisotropy is significantly lower than our present value. Diffusion measurements on impurity molecules, generally, underestimate the diffusion anisotropy of the solvent, even where the guest molecule closely matches the mass and geometry of the host molecule [41–44,55,56]. Moreover, the relation between average diffusion coefficients in nematic phase and $D_{iso}$ is am-

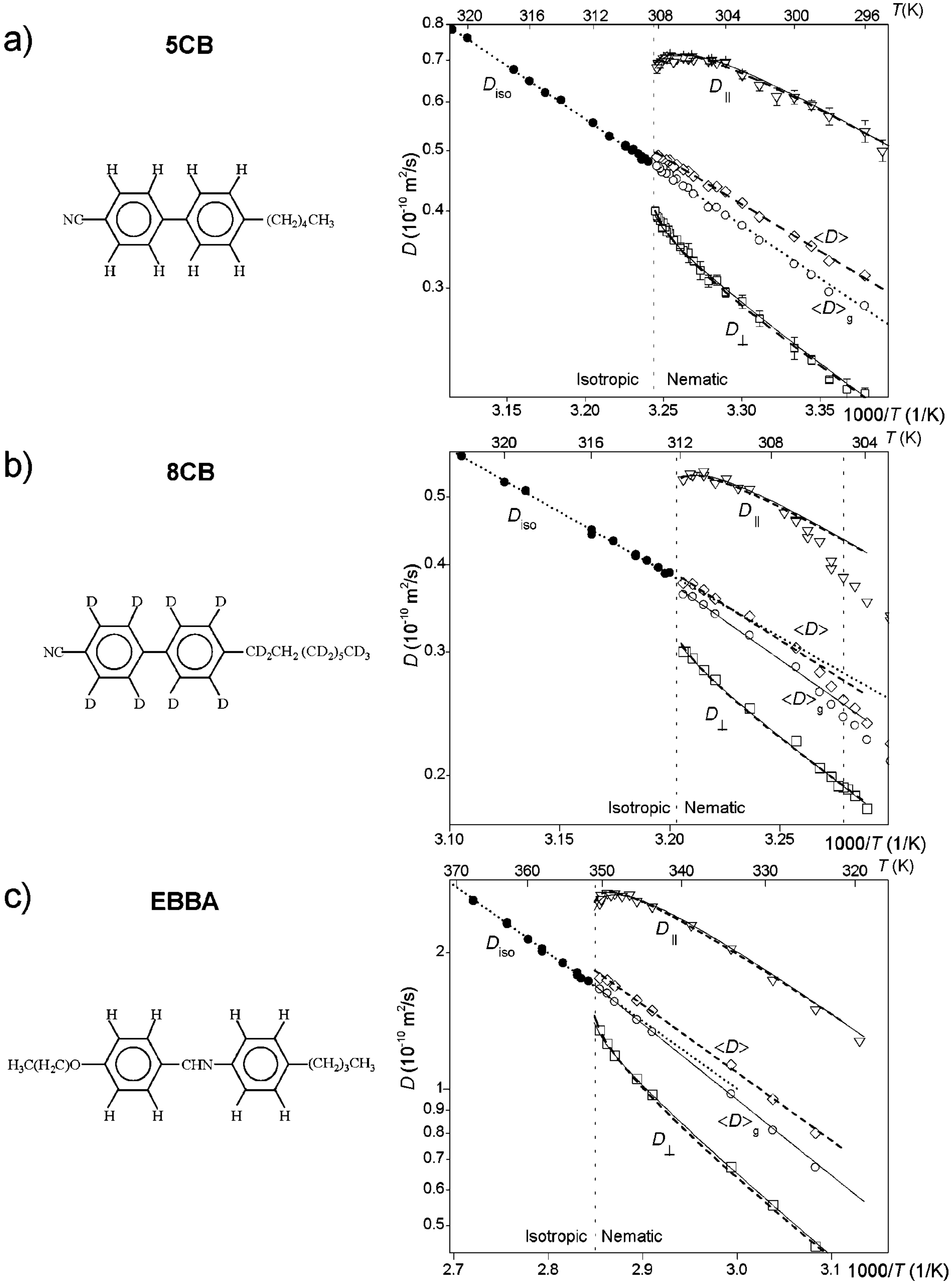

FIG. 1. The temperature dependence of the diffusion coefficient $D_{iso}$ (●) in the isotropic phase and principal diffusion coefficients $D_\perp$ (□) and $D_\parallel$ (▽) in the nematic liquid crystal. Their averages, $\langle D\rangle=(2D_\perp+D_\parallel)/3$ (◇) and $\langle D\rangle_g=(D_\perp)^{2/3}(D_\parallel)^{1/3}$ (○), are also included. The dotted lines are the Arrhenius fits to the isotropic diffusion coefficient $D_{iso}$, also extrapolated into the mesophase region. Dashed and solid lines are the fits to the CM model [30] [Eqs. (1)] and to the HFA model [31] [Eqs. (2)], respectively.

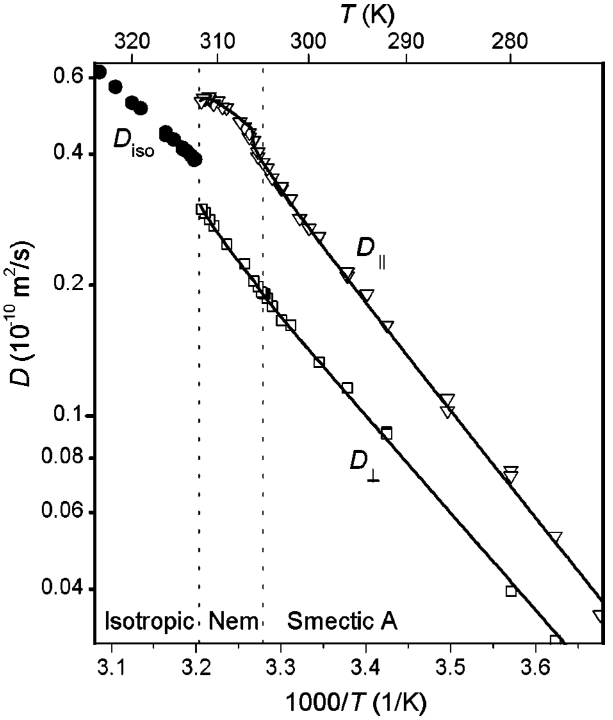

FIG. 2. Experimental diffusion data $D_{\perp}$ (□) and $D_{\parallel}$ (▽) in the nematic and smectic-*A* phases of 8CB together with theoretical fits (lines). $D_{iso}$ (●) is the diffusion coefficient in the isotropic phase. In the nematic phase the HFA model [31] is applied with parameters as in Fig. 1(b). In the smectic phase and near the phase transition in the nematic phase the modified Volino and co-author's model [33,34] [Eqs. (4),(5)] with the potential amplitude given in Eq. (6) is applied.

biguous in this case. The results by QENS in nematic chain-deuterated EBBA [57–59], available only for nominally perpendicular direction, disagree with our results by a factor of $\approx 2$ in magnitude (after the correction for temperature shift and presumably inhomogeneous sample orientation [57]). The activation energy, however, agrees well.

The temperature dependence of diffusion coefficients within the mesophase can be tentatively decomposed in a conventional *thermally activated* Arrhenius-type process, analogous to one observed in the isotropic phase, and an *anisotropy activated* process due to the presence of molecular orientational ordering. The nematic diffusion models of Refs. [30,31] (see Sec. III) deal with the latter (anisotropic) contribution. Inspection of the temperature dependences of the average diffusion coefficients reveals that the parameters of thermally activated contribution are similar to that in the isotropic phase. Note that various theoretical models introduce different average diffusion coefficients (see above). However, for small diffusion anisotropy their difference is not significant (Fig. 1) and isotropic and geometric averages, $\langle D\rangle$ and $\langle D\rangle_g$, are within 5–10 % of the diffusion coefficients extrapolated from the isotropic phase. Also, the apparent activation energies are of similar magnitude.

In the models, the theoretical "diffusion coefficient in the isotropic limit" is formally defined as the limiting value of $D_{\parallel,\perp}$ at $S\rightarrow 0$. Since $S=0$ implies that the sample is converted to its isotropic liquid state, this limiting diffusion coefficient is expected to coincide with, or to be close to, the value extrapolated from the isotropic phase.

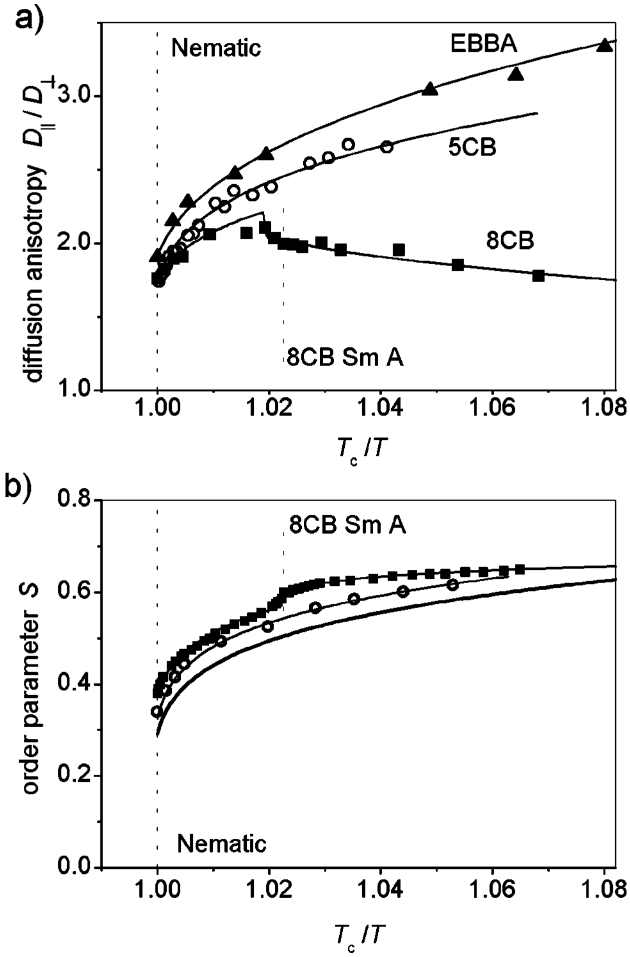

FIG. 3. The temperature dependence of the diffusion anisotropy $D_{\parallel}/D_{\perp}$ in 5CB (○), 8CB (■), and EBBA (▲). Solid lines are calculated using the HFA model (for 5CB and EBBA) and the combined HFA and Volino and co-author's models (for 8CB) with the parameters as in Figs. 1 and 2. (b) The temperature dependence of the order parameter *S* in 5CB (○), 8CB (■), and EBBA (bold line) as reported in Refs. [60–62], respectively. Thin lines are the approximation by Haller function [63], as described in the text.

Interpreting the experimental data in terms of the models requires the knowledge of the order parameter profile across the mesophase region. Since it was not determined in the present work, we rely on literature data. Fortunately, for the present samples numerous measurements of *S* have been reported. Data typically scatter within approximately 20% wide ranges due to experimental scaling problems. The relative profiles, however, are much more accurate. In our simulations, we selected (somewhat arbitrarily) the order parameter profiles of Refs. [60–62] for 5CB, 8CB, and EBBA, respectively, that fall approximately in the middle of scattering intervals. The data, presented in Fig. 3(b), in the nematic phases were approximated by the Haller function $S_{nem}=(1-T/T^{*})^{\gamma}$ [63] with the parameters values $T^{*}=308.5$ K and $\gamma=0.162$, $T^{*}=312.5$ K and $\gamma=0.150$, $T^{*}=351.4$ K and $\gamma=0.182$, for samples 5CB, 8CB, and EBBA, respectively.

TABLE I. Parameters for the diffusion model simulation in the isotropic and nematic phases.

| | Isotropic | Nematic phase | | | |
|---|---|---|---|---|---|
| | | CM model | | HFA model | |
| | $E_a^{iso}$ (kJ/mol) [b] | $E_a^{\langle D\rangle}$ (kJ/mol) [c] | $Q$ [a] | $E_a^{\langle D\rangle_g}$ (kJ/mol) [c] | $Q$ [a] |
| 5CB | 32.8 | 29.1 | 4.4<br>(3.6–5.6) | 32.8 | 2.4<br>(2.2–2.6) |
| 8CB | 34.2 | 38.3 | 3.4<br>(2.9–3.9) | 42.4 | 2.1<br>(1.9–2.2) |
| EBBA | 28.7 | 28.7 | 6.6<br>(5.2–9.2) | 32.0 | 2.9<br>(2.5–3.4) |

[a] Values in parentheses are the range of variation of the best fit value of $Q$ when the order parameter $S$ is scaled by a factor of 0.9–1.1 corresponding to the scatter in the previously determined experimental order parameter.

[b] $(\pm 0.5)$ kJ/mol.

[c] $(\pm 2.0)$ kJ/mol.

In the smectic-$A$ phase of 8CB the approximation $S_{sm} = 0.721 \times (1 - T/306.07)^{0.033}$ was used.

*CM model [30]*. The two sets of diffusion coefficients, $D_\perp$ and $D_\parallel$, were numerically fitted to Eqs. (1a),(1b) with the axial ratio $Q$ as the only free parameter. The activation energy $E_a^{\langle D\rangle}$, required in the model, was determined from the slope of the experimental $\langle D\rangle$ temperature dependence (Fig. 1). Note that for 8CB, the points in the nematic phase close to the smectic transition temperature, where formation of pretransitional smectic clusters may influence the diffusion coefficient, were excluded from the fit. The values of $Q$, derived from the analysis, together with the activation energies $E_a^{\langle D\rangle}$ are collected in Table I and the results are shown in Fig. 1. A number of observations can be pointed out:

(i) The isotropic average $\langle D\rangle = (2D_\perp + D_\parallel)/3$ in the nematic phase can be described by the Arrhenius-type relationship, except for the phase transition region. In 5CB and EBBA samples, a small but significant discontinuity for coefficient $\langle D\rangle$ is observed at the nematic-isotropic transition, so that $\langle D\rangle$ is approximately 5% larger compared to the isotropic diffusion coefficient $D_{iso}$ near the transition point. No such discontinuity was detected within experimental accuracy for 8CB.

(ii) No obvious trend is observed for the activation energies in nematic liquid crystals compared to the isotropic phases. In fact, these are slightly lower, slightly higher, and unaffected for 5CB, 8CB, and EBBA, respectively. This is in agreement with the expectations since the activation energies in the nematic phases reflect the temperature behavior of a hypothetical isotropic diffusion coefficient, $\langle D\rangle$.

(iii) The axial ratios $Q$ determined for the three compounds are larger than expected from the molecular geometries $(Q \approx 3)$. In particular the value derived for EBBA $(Q = 6.6)$ is in contradiction with the molecular picture.

*HFA model [31]*. In analogy with the CM model analysis, the diffusion coefficients $D_\perp$ and $D_\parallel$ were fitted to Eqs. (2a)–(2c) using the axial ratio $Q$ as free parameter and with the activation energy $E_a^{\langle D\rangle_g}$ determined from the slope of the experimental $\langle D\rangle_g$ temperature dependence. Also here, the points in the nematic-smectic transition region (for 8CB sample) were excluded from the fit. The values of $Q$, derived from the analysis, and the activation energies for $\langle D\rangle_g$ are included in Table I and results are shown in Fig. 1. The conclusions from the analysis can be summarized as follows:

(i) The geometrical average $\langle D\rangle_g$ calculated from the experimental diffusion coefficients $D_\parallel$ and $D_\perp$ using Eq. (2d) coincides with the line extrapolated from the isotropic phase (Fig. 1). This agreement is particularly impressive for 5CB.

(ii) Once again we note that the activation energies for the average diffusion coefficient are similar to those determined in the isotropic phase.

(iii) The axial ratio parameters derived here are essentially in agreement with the values we expect from molecular geometries $(Q \approx 3)$. Somewhat low values for 5CB and 8CB may be a consequence of molecular association as was suggested from x-ray data for 5CB [36,64]. In a similar type of experiment on EBBA homologs no association phenomenon has been observed [64]. The smaller axial ratio for 8CB as compared to 5CB homolog can be explained by the fact that the longer chain inclined to the molecular core results in increasing the effective molecular diameter. Note that, the $Q$ values for $n$CB are very similar to those recently obtained from the analysis of the viscosity data: $Q = 2.6$ and 1.9 for 5CB and 8CB, respectively [65].

*Franklin model [32]*. The analysis using this model requires the five Leslie coefficients $\alpha_i$ $(i = 1, \ldots, 5)$ and the scalar friction constants $f$ in the nematic phase, which are scarcely available. The complete and relatively accurate set of Leslie coefficients can only be found for 5CB, as reported in Ref. [66]. Hence, analysis of diffusion in this sample only will be considered. However, accurate value of the friction constant $f$ and its temperature dependence is still missing. Therefore the difference of two diffusion coefficients $(D_\parallel - D_\perp)$ was evaluated, since in that the term containing $f$ is canceled out [cf. Eqs. (3)]. The calculated and experimental data are compared in Fig. 4. A clear disagreement in quali-

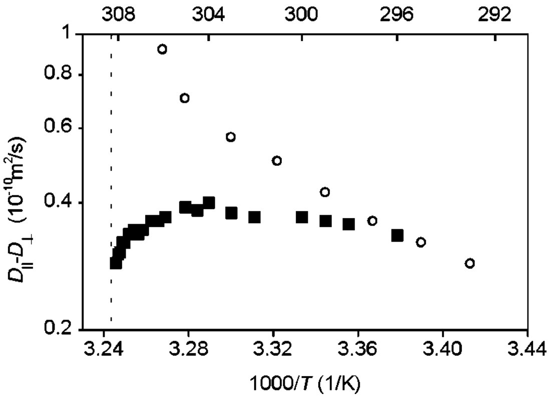

FIG. 4. Comparison of the experimental difference of two principal diffusion coefficients ($D_{\|}-D_{\perp}$) (■) in nematic 5CB to the calculation (○) by the Franklin model [32] of Eq. (3).

tative behavior is seen. This theory is based on the analogy with polymer solutions in which the number of flexible segments in the molecule is supposed to be large, which is obviously not the case for 5CB molecule. Alternatively, the inconsistence may also be caused by insufficient accuracy of experimental Leslie coefficients, especially in the phase transition region.

### B. Smectic-*A* phase

Measurements of molecular diffusion in smectic phases have been reported more frequently in the literature as compared to nematics. The ability of a viscous smectic phase to keep its director orientation at an arbitrary angle to the magnetic field allowed performing conventional PGSE NMR experiment with the director oriented at the "magic angle" 54.7° to the magnetic field. In such a situation, the nuclear dipolar couplings are suppressed [1,67–70]. This type of experiment, however, is not feasible for 8CB due to a relatively fast director reorientation characteristic of the smectic phase of this compound [71].

In 8CB, the relation $D_{\|}>D_{\perp}$ characteristic of nematics, holds also in the smectic-*A* phase (Fig. 2). This result is in contradiction with theoretical expectations [1,20,33,34,39,72] and also with the majority of experimental results in other compounds. Such unconventional behavior, however, has previously been observed in cyanobenzylidene-octyloxyaniline (CBOOA) [70] and terephthal-bis-butylaniline (TBBA) [68]. Also, recent molecular dynamics simulation of the smectic-*A* phase of 8CB (though, performed only on nanosecond time scale) predicted $D_{\|}>D_{\perp}$ [73]. The fact that the smectic layer structure is stable in spite of faster out-of-layer diffusion $D_{\|}$ compared to in-layer motion $D_{\perp}$ has been discussed in the literature [74] and can be understood by assuming solid-like jump process diffusion for $D_{\|}$ and liquidlike small step (compared to molecular sizes) diffusion inside the layer. In contrast to nematics, the apparent activation energy in the smectic phase is larger for diffusion parallel to director (i.e., along the smectic layers normal), $E_a^{\|}>E_a^{\perp}$. Hence, if the smectic-phase temperature region would extend to lower temperatures, the two curves $D_{\|}(T)$ and $D_{\perp}(T)$ would cross, resulting in a more "conventional" behavior with faster in-layer diffusion. This has indeed been observed in smectic-*A* phase of TBBA [68].

Another notable experimental result in 8CB is the *continuous* decrease of both principal diffusion coefficients observed at the nematic-smectic phase transition. On the other hand, the diffusion anisotropy behavior changes from a general increase with lowering temperature in nematic phase to the opposite in smectic phase [Fig. 3(a)]. Note, that the theoretical model [33,34,39] predicts discontinuity of $D_{\|}$ and its activation energy at the nematic-smectic transition as a result of layered structure formation. By experiments, previous measurements were of insufficient accuracy near the transition point [1,39,68,69].

The analysis of the diffusion coefficients using the Volino *et al.* model [Eqs. (4),(5)] resulted in large fitting errors and unphysical parameters. Therefore, in order to adapt the model to a situation with continuous change of diffusion coefficients at the nematic-smectic transition we empirically modified it by allowing the parameter $V_1$ in Eq. (4) to become temperature dependent. Suitably parametrized form of function $V_1(T)$ is

$$V_1=V_0(1-T/T^*)^{\gamma}, \tag{6}$$

which reflects the temperature dependence of McMillan's smectic order parameter [75]. The value of parameter $T^*$ in Eq. (6) is close to the smectic-nematic transition temperature and $V_0$ is the potential amplitude at the low-temperature limit. The modified model converges to the original expressions of Eqs. (4),(5) at temperatures within the smectic phase away from the transition point, where the potential of Eq. (6) becomes virtually constant.

The experimental results in 8CB in its smectic phase and in pre-transitional region in nematic phase were simulated by Eqs. (4)–(6), where the coefficients $(D_{\|})^{nem}$ and $(D_{\perp})^{nem}$ are calculated according to the HFA model with the parameters optimized in the nematic phase of 8CB (see above). The best parameters for the potential of Eq. (6) are estimated to $V_0=6.5$ kJ/mol, $T^*=306.13$ K, and $\gamma=0.150$. The potential amplitude can be compared to the values 4.6 and 11.1 kJ/mol, obtained for TBBA [33,34] and ethyl-acetoxybenzylidene-aminocinnamate (EABAC) [1], respectively. The corresponding fit for both the nematic and smectic regions, shown in Fig. 2, demonstrates a good consistency with the experiment. Particularly, it was possible to fit the theory to the data in the nematic–smectic-*A* phase transition region.

## V. CONCLUSION

We have presented the measurements of diffusion coefficients for three mesogenic compounds (5CB, 8CB, and EBBA) in their isotropic and liquid crystalline (nematic and smectic-*A*) phases. The methods, based on $^1$H and $^2$H PGSE NMR, allow accurate measurements of diffusion coefficients in the range down to $10^{-12}$ m$^2$/s. The measurements provided information on anisotropic diffusion that was previously inaccessible.

Since the self-diffusion of the molecules constituting the mesophase is measured instead that of probe molecules, the information is direct and the analysis and interpretation is simple. In the nematic phase, three different models were applied to experimental diffusion coefficients: (i) *the Chu-Moroi model* where the self-diffusion coefficient has been derived using a parametrized form of the linear momentum time autocorrelation function [30], (ii) *the Hess-Frenkel-Allen* approach based on the affine transformation from the isotropic diffusion of hard spheres to the space of aligned uniaxial ellipsoids [31], and (iii) *the Franklin model* that rests on the hydrodynamic theory for isotropic liquids [32]. All three models depend on parameters that are related to the orientational order and molecular shape. In the analyses we performed numerical fits of the experimental diffusion coefficients, $D_\perp$ and $D_\parallel$. The analysis using the hydrodynamic model (iii) failed completely. Models (i) and (ii) were, on the other hand, able to provide fits with reasonable parameter values. In fact, the latter produced very realistic molecular axial ratios for all three compounds.

For the first time the transformation of the diffusion tensor at the nematic–smectic-*A* transition is accurately measured. It is found that for the 8CB sample the diffusion coefficients change continuously and ‘‘nematic-like’’ relation $D_\parallel > D_\perp$ persists in the observed smectic temperature range. The translational dynamics in the smectic-*A* phase of 8CB can be described by Volino and co-authors' model [33,34], modified for the case of the second-order nematic-smectic phase transition.

## ACKNOWLEDGMENTS

This work has been supported by the Carl Tryggers Foundation, Magn. Bergvalls Foundation, the Swedish Research Council (VR), and the Deutscher Academischer Austauschdienst together with the Swedish Institute under Project No. 313-S-PPP-7/98.

[1] G. J. Krüger, Phys. Rep. **82**, 229 (1982).
[2] F. Noack, Mol. Cryst. Liq. Cryst. **113**, 247 (1984).
[3] J. Kärger, H. Pfeifer, and W. Heink, Adv. Magn. Reson. **12**, 1 (1988).
[4] F. Noack, St. Becker, and J. Struppe, Annu. Rep. NMR Spectrosc. **33**, 1 (1997).
[5] F. Noack, in *Handbook of Liquid Crystals*, edited by D. Demus *et al.* (Wiley-VCH, Weinheim, 1998), Vol. 1, Chap. 13.
[6] S. Miyajima, EMIS Datarev. Ser. **25**, 457 (2000).
[7] S. V. Dvinskikh, R. Sitnikov, and I. Furó, J. Magn. Reson. **142**, 102 (2000).
[8] S. V. Dvinskikh and I. Furó, J. Magn. Reson. **144**, 142 (2000).
[9] S. V. Dvinskikh and I. Furó, J. Magn. Reson. **146**, 283 (2000).
[10] S. V. Dvinskikh and I. Furó, J. Magn. Reson. **148**, 73 (2001).
[11] S. V. Dvinskikh and I. Furó, J. Chem. Phys. **15**, 1946 (2001).
[12] S. V. Dvinskikh *et al.*, J. Magn. Reson. **153**, 83 (2001).
[13] E. O. Stejskal and J. E. Tanner, J. Chem. Phys. **42**, 288 (1965).
[14] J. E. Tanner, J. Chem. Phys. **52**, 2523 (1970).
[15] P. Stilbs, Prog. Nucl. Magn. Reson. Spectrosc. **19**, 1 (1987).
[16] P. T. Callaghan, in *Principles of Nuclear Magnetic Resonance Microscopy* (Clarendon Press, Oxford, 1991).
[17] W. S. Price, Concepts Magn. Reson. **9**, 299 (1997).
[18] W. S. Price, Concepts Magn. Reson. **10**, 197 (1998).
[19] R. Blinc, J. Pirš, and I. Zupančič, Phys. Rev. Lett. **30**, 546 (1973).
[20] R. Blinc *et al.*, Phys. Rev. Lett. **33**, 1192 (1974).
[21] I. Zupančič *et al.*, Solid State Commun. **15**, 227 (1974).
[22] M. S. Crawford, B. C. Gerstein, A.-L. Kuo, and C. G. Wade, J. Am. Chem. Soc. **102**, 3728 (1980).
[23] I. Chang *et al.*, Phys. Rev. Lett. **76**, 2523 (1996).
[24] Wurong Zhang and D. G. Cory, Phys. Rev. Lett. **80**, 1324 (1998).
[25] S. V. Dvinskikh, I. Furó, H. Zimmermann, and A. Maliniak, Phys. Rev. E (to be published).
[26] H. Zimmermann, Liq. Cryst. **4**, 591 (1989).
[27] D. Demus and H. Zaschke, in *Flüssige kristalle in Tabellen II* (VEB Deutscher Verlag für Grundstoffindustrie, Leipzig, 1984).
[28] I. Furó and H. Johannesson, J. Magn. Reson., Ser. A **119**, 15 (1996).
[29] R. Mills, J. Phys. Chem. **77**, 685 (1973).
[30] K.-S. Chu and D. S. Moroi, J. Phys. (Paris), Colloq. **36**, C1-99 (1975).
[31] S. Hess, D. Frenkel, and M. P. Allen, Mol. Phys. **74**, 765 (1991).
[32] W. Franklin, Phys. Rev. A **11**, 2156 (1975).
[33] F. Volino, A. J. Dianoux, and A. Heidemann, J. Phys. (France) Lett. **40**, L583 (1979).
[34] F. Volino and A. J. Dianoux, Mol. Phys. **36**, 389 (1978).
[35] W. Urbach, H. Hervet, and F. Rondelez, J. Chem. Phys. **83**, 1877 (1985).
[36] A. J. Leadbetter, F. P. Temme, A. Heidemann, and W. S. Howells, Chem. Phys. Lett. **34**, 363 (1975).
[37] K. Ohta, M. Terazima, and N. Hirota, Bull. Chem. Soc. Jpn. **68**, 2809 (1995).
[38] M. P. Allen, Phys. Rev. Lett. **65**, 2881 (1990).
[39] R. M. Richardson, A. J. Leadbetter, D. H. Bonsor, and G. J. Krüger, Mol. Phys. **40**, 741 (1980).
[40] G. J. Krüger and H. Spiesecke, Z. Naturforsch. A **28**, 964 (1973).
[41] M. Hara, S. Ichikawa, H. Takezoe, and A. Fukuda, Jpn. J. Appl. Phys., Part 1 **23**, 1420 (1984).
[42] M. Hara *et al.*, Jpn. J. Appl. Phys., Part 2 **24**, L777 (1985).
[43] M. Hara, H. Takezoe, and A. Fukuda, Jpn. J. Appl. Phys., Part 1 **25**, 1756 (1986).
[44] H. Takezoe, M. Hara, S. Ichikawa, and A. Fukuda, Mol. Cryst. Liq. Cryst. **122**, 169 (1985).
[45] T. Nishikawa, J. Minabe, H. Takezoe, and A. Fukuda, Mol. Cryst. Liq. Cryst. **231**, 153 (1993).
[46] R. Blinc, B. Marin, J. Pirš, and J. W. Doane, Phys. Rev. Lett. **54**, 438 (1985).
[47] G. Rollmann, K. F. Reinhart, and F. Noack, Z. Naturforsch. A **34**, 964 (1979).
[48] S. K. Ghosh, E. Tettamanti, and A. Ricchiuto, Chem. Phys. Lett. **101**, 499 (1983).

[49] M. E. Moseley and A. Loewenstein, Mol. Cryst. Liq. Cryst. **90**, 117 (1982).

[50] S. K. Ghosh and E. Tettamanti, Lett. Nuovo Cimento Soc. Ital. Fis. **40**, 197 (1984).

[51] M. Vilfan *et al.*, J. Chem. Phys. **103**, 8726 (1995).

[52] P. Holstein *et al.*, J. Magn. Magn. Mater. **143**, 427 (2000).

[53] N. V. Kashirin, V. D. Skirda, and I. V. Ovchinnikov, Colloid J. **62**, 68 (2000).

[54] M. Vilfan *et al.*, Magn. Reson. Imaging **19**, 433 (2001).

[55] D. R. Spiegel, A. L. Thompson, and W. C. Campbell, J. Chem. Phys. **114**, 3842 (2001).

[56] H. Hervet, W. Urbach, and F. Rondelez, J. Chem. Phys. **68**, 2725 (1978).

[57] M. P. Fontana, M. Ricco, C. J. Carlile, and B. Rosi-Schwartz, Physica B **180-181**, 726 (1992).

[58] M. Ricco *et al.*, Mol. Cryst. Liq. Cryst. **212**, 139 (1992).

[59] M. P. Fontana and G. Gallone, Phys. Scr. **T57**, 168 (1995).

[60] J. W. Emsley, G. R. Luckhurst, and C. P. Stockley, Mol. Phys. **44**, 565 (1981).

[61] R. G. Horn, J. Phys. (Paris) **39**, 105 (1978).

[62] M. Ylihautala, J. Lounila, and J. Jokisaari, J. Chem. Phys. **110**, 6381 (1999).

[63] I. Haller, Prog. Solid State Chem. **10**, 103 (1975).

[64] A. J. Leadbetter, R. M. Richardson, and C. N. Colling, J. Phys. (Paris), Colloq. **36**, C1-37 (1975).

[65] H. Ehrentraut and S. Hess, Phys. Rev. E **51**, 2203 (1995).

[66] H. Herba, A. Szymanski, and A. Drzymala, Mol. Cryst. Liq. Cryst. **127**, 153 (1985).

[67] G. J. Krüger, H. Spiesecke, and R. Weiss, Phys. Lett. **51A**, 295 (1975).

[68] G. J. Krüger, H. Spiesecke, and R. V. Steenwinkel, J. Phys. (Paris), Colloq. **37**, C3-123 (1976).

[69] G. J. Krüger, H. Spiesecke, R. V. Steenwinkel, and F. Noack, Mol. Cryst. Liq. Cryst. **40**, 103 (1977).

[70] S. Miyajima, A. F. McDowell, and R. M. Cotts, Chem. Phys. Lett. **212**, 277 (1993).

[71] J. W. Emsley, J. E. Long, G. R. Luckhurst, and P. Pedrielli, Phys. Rev. E **60**, 1831 (1999).

[72] O. Parodi, J. Phys. (France) Lett. **37**, L-143 (1976).

[73] Y. Lansac, M. A. Glaser, and N. A. Clark, Phys. Rev. E **64**, 051703 (2001).

[74] G. J. Krüger and R. Weiss, J. Phys. (Paris) **38**, 353 (1977).

[75] W. L. McMillan, Phys. Rev. A **4**, 1238 (1971).

[76] S. V. Dvinskikh (unpublished).